A Convective-Diffusion Model for Dissolution of Two Non-interacting Drug Mixtures from Co-compressed Slabs Under Laminar Hydrodynamic Conditions

Seshadri Neervannan,[1] Lloyd S. Dias,[2] Marylee Z. Southard,[3] and Valentino J. Stella[1,4]

Received August 5 1993; accepted March 29, 1994

A numerical convective-diffusion dissolution model has been extended to describe dissolution of two neutral non-interacting drugs co-compressed in a slab geometry. The model predicted the experimental dissolution rates of naproxen/phenytoin mixtures and hydrocortisone/nitrofurantoin mixtures quite accurately, except for phenytoin in the naproxen/phenytoin mixture at low weight proportions. A non-linear dependence of dissolution rate on weight proportion with a positive deviation from linearity was observed. An increase in flow rate increased the dissolution rate and the cube-root dependency of dissolution rate on the flow rate for a given weight proportion of the component in the slab, as proposed earlier by Shah and Nelson for pure compounds, was also observed here, suggesting that the changes in dissolution profile were caused by changes in surface area only. As expected from the model an increase in particle size of the powders used to make the slab decreased the dissolution rate. This was explained by an increase in the average length of the component resulting in a bigger 'carryover' of material from one section of the component in the slab to the next section of the same component, due to convection, and hence lower flux.

KEY WORDS: convective diffusion; co-compressed slab; carryover; dissolution; laminar flow; numerical model; particle size.

INTRODUCTION

The oral absorption of poorly soluble drugs can be limited by the rate of dissolution from dosage forms due to the composition and the hydrodynamics of the environment in the gastrointestinal (GI) tract. The mechanism of dissolution of pure ionizable and neutral compounds has been investigated quite extensively (1–5). However, the dissolution of drugs when co-compressed with other excipients, inert or otherwise, has not been quantitatively studied. Some models have been proposed for the dissolution of multi-component systems for non-interacting as well as interacting components, from non-disintegrating spheres (6–9). The models were based on simple diffusion layer theory according to the Noyes-Whitney law, and a diffusion-controlled mechanism was assumed. The common premises in all these models were that the dissolution rate of a component depends on the relative surface area available to that component and that the contribution of fluid flow to dissolution can be excluded. These models provide a general understanding of the dependence of dissolution rates on the relative surface area and the drug diffusion coefficients. Recent work has established that the hydrodynamics, or fluid flow, surrounding the tablet play an important role in drug dissolution and hence cannot be excluded (4,5,10).

The hydrodynamic patterns in the GI tract vary with fed and fasted states; thus it is not possible to simulate the fluid motion exactly. However, it has been shown that laminar flow exists in the upper GI tract, which is the environment through which materials diffuse to reach absorption sites (11). Also, it is believed that laminar flow is an accurate approximation of the semi-stagnant micro-environment surrounding the dissolving drug surface regardless of its location in the GI tract or stomach (12).

A laminar flow dissolution apparatus was reported and evaluated (13,14). For ease of computation, the authors assumed a linear velocity profile in the device instead of the parabolic profile that is characteristic of the laminar flow across a flat surface (15). A mathematical model was written to calculate dissolution rates in the apparatus. Although that model predicted experimental data quite accurately for slabs containing pure neutral compounds, it could not be extended to include other interactions such as ionization reactions and co-compression of multiple components. In a more recent study, a numerical convective-diffusion model was proposed which incorporated the actual parabolic velocity profile to characterize the laminar flow hydrodynamics (16). While the numerical model predicted the experimental results as accurately as the earlier analytical model, it could also be extended to include other interactions.

In the present study, a numerical convective-diffusion model was derived to describe the dissolution of two non-interacting neutral compounds when they are co-compressed together at various weight proportions. The model results were compared with the experimental dissolution rates of non-interacting drug mixtures such as naproxen (I) with phenytoin (II) and hydrocortisone (III) with nitrofurantoin (IV) (Fig. 1) as a function of various weight proportions and particle sizes as well as flow rate in the laminar flow system in order to elucidate the mechanisms that control the dissolution process.

MODEL DEVELOPMENT AND SOLUTION METHODS

The present model simulates dissolution rates of two non-interacting compounds which are co-compressed into a rectangular slab. Because the dissolving surface is not uniform in composition, the fraction of a typical compound in the total formulation and its particle size will affect its dissolution rate. The composition and dynamics of the dissolution medium are also major factors. Hence, the current model was developed to determine accurately the dependence of dissolution rate on relative surface area exposed to a well-characterized dissolution medium.

Determination of Average Particle Lengths

In this study, a solid granular mixture of two compounds

[1] Department of Pharmaceutical Chemistry, The University of Kansas, Lawrence, Kansas 66045.
[2] Abbott Laboratories, 1400 Sheridan Road, North Chicago, Illinois 60064.
[3] Department of Chemical and Petroleum Engineering, The University of Kansas, Lawrence, Kansas 66045
[4] To whom correspondence should be addressed.

0724-8741/94/0900-1288$07.00/0

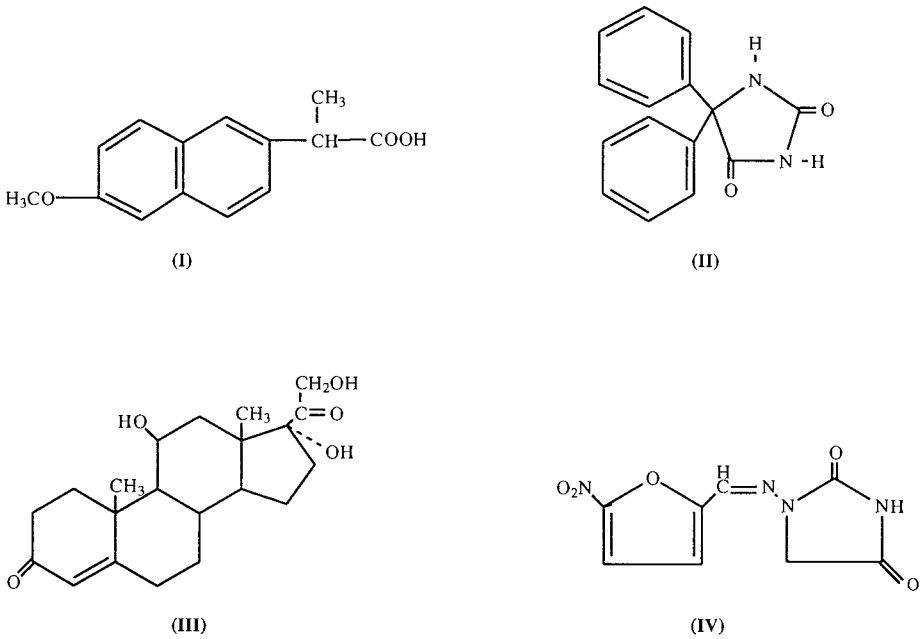

Figure 1 List of model compounds used in the dissolution study; (I) naproxen, (II) phenytoin, (III) hydrocortisone and (IV) nitrofurantoin.

A and B is blended and compressed. Sieve grading was used to yield equal and narrow particle size ranges of both components. It is assumed that neither compound interacts with the other in any way, either in solid phase or in solution. The dissolution rate of B in the slab is affected by the presence of A only because the surface area ratio of the two compounds is changed. For example, at low weight proportion of A in the slab, it is unlikely that two particles of A touch each other. As the proportion of A is increased, it is statistically more likely that some particles of A will align themselves together, and the average length of A particles on the slab surface will be greater than that of a single particle of A. A statistical Monte Carlo technique (17) was utilized to determine a probable average component length of A and B on the surface corresponding to their weight proportion.

The Monte Carlo simulation method uses a random number generator to determine the frequency of particles of a certain type appearing next to each other. Depending on the surface area ratio of compounds, the random numbers are assigned as compound A or B. The sequence of the two compounds is monitored to determine the number of repeating units and an average component length of the repeating unit of each compound is calculated (18). As depicted in Figure 2, the components A and B with the average lengths of L1 and L2, respectively, and a width of b (the width of the slab), are assumed to be aligned alternately on the surface of the slab. The results from this statistical method are listed in Table I, where the average number of like particles which align together is given. The lengths L1 and L2 are calculated by multiplying this average particle number by the particle size. For example, a 67:33 mixture of A:B having a nominal particle size of 335 μm would have an average A length (L1) of 1015 μm and a B length (L2) of 499 μm.

Transport Equations and Boundary Conditions

The convective-diffusion dissolution model described earlier (14,16) has been extended here. It is assumed that mass transport occurs by bulk flow (convection) in the direction of fluid flow (x) and by diffusion in the direction perpendicular to the dissolving surface (y). The transport equations incorporating these mechanisms are derived for

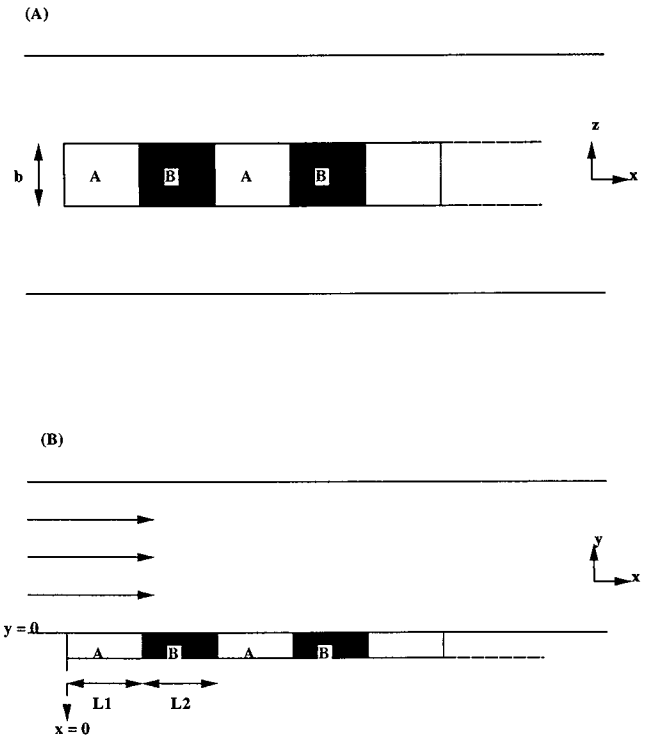

Figure 2 Partial representation of the co-compressed pellet in the laminar dissolution apparatus showing the repeating units of A and B with lengths L1 and L2 respectively and width b. (A) Top view (B) Side view. The fluid flow is in x-direction.

TABLE I. The results from the Monte-Carlo simulation technique for a random mixture of A and B (Mean ± SEM, n = 50000). It was assumed that not more than 20 particles of a single component align next to each other.

Ratio of A to B	Average length of A[a]	Average length of B[a]
10:90	$1.10 \pm 5.2 \times 10^{-3}$	7.20 ± 0.03
25:75	$1.33 \pm 3.5 \times 10^{-3}$	$3.96 \pm 9.0 \times 10^{-3}$
33:67	$1.49 \pm 7.2 \times 10^{-4}$	$3.03 \pm 6.0 \times 10^{-3}$
50:50	$2.00 \pm 2.2 \times 10^{-3}$	$2.00 \pm 2.2 \times 10^{-3}$
67:33	$3.03 \pm 5.8 \times 10^{-3}$	$1.49 \pm 7.3 \times 10^{-3}$
75:25	$3.96 \pm 8.9 \times 10^{-3}$	$1.33 \pm 3.6 \times 10^{-3}$
90:10	$7.20 \pm 9.2 \times 10^{-3}$	$1.10 \pm 4.9 \times 10^{-5}$

[a] The length indicates the average number of similar particles that are aligned next to each other. The actual length is calculated by multiplying the length with the average particle size.

compounds A and B separately, since they are assumed to be non-interacting, as given in Equation 1:

$$\frac{\partial C_A}{\partial t} = D_A \frac{\partial^2 C_A}{\partial y^2} - V_x \frac{\partial C_A}{\partial x}$$
$$\frac{\partial C_B}{\partial t} = D_B \frac{\partial^2 C_B}{\partial y^2} - V_x \frac{\partial C_B}{\partial x} \quad (1)$$

The velocity term, V_x, was described with a parabolic function with y as a variable and taking an average velocity in the z dimension (16). Diffusion in x and z directions were assumed to be negligible and hence were not included in the present model. The corresponding boundary conditions for the above governing equations are described as below for a single repeating unit of A and B (Fig. 2):

$$C_A = C_{A,o}, \text{ for } 0 < x < L1 \text{ at } y = 0 \quad (1a)$$
$$C_B = C_{B,o}, \text{ for } L1 < x < L2 \text{ at } y = 0 \quad (1b)$$
$$\frac{\partial C_A}{\partial y} = 0 \text{ for } L1 < x < L2 \text{ at } y = 0 \quad (1c)$$
$$\frac{\partial C_B}{\partial y} = 0 \text{ for } 0 < x < L1 \text{ at } y = 0 \quad (1d)$$
$$C_A = C_B = 0 \text{ at } y = Y \text{ for all } x \quad (1e)$$
$$C_A = C_B = 0 \text{ at } x = 0 \text{ for all } y \quad (1f)$$

where, $C_{A,o}$ and $C_{B,o}$ are the intrinsic solubilities and L1 and L2 are component lengths of A and B respectively. Equations 1a and 1b represent saturated solubility conditions at the respective surfaces of A and B. Equations 1c and 1d represent no-flux conditions, wherein there is no flux of A from a section of the slab occupied by B, and vice versa. Equations 1e and 1f represent sink conditions at regions far removed from the dissolving surface.

Numerical Solution Method

The system of equations described above was solved numerically using finite difference approximations as described elsewhere (5,19). Implicit differences were used to approximate the partial derivatives by expressing all positional derivatives at a new time step, instead of the explicit differences, in order to minimize computing time and the instability of the numerical routine (19,20). The concentrations were calculated for each repeating unit of A and B, (a) by proceeding along the x-direction; (b) by applying the transport equations for all points perpendicular to the surface (in the y direction) at that x; and (c) solving the resulting simultaneous difference equations (5). The y-step size, Δy, was kept constant for all formulations, while the x-step size, Δx, was changed depending on the ratio of A to B.

When the solution converged to steady state, where the fractional change in concentration with respect to time is less than a given value (usually 1×10^{-5}), the dissolution rates of A and B were determined by calculating the flux at the respective surfaces of A and B on the slab and multiplying it by the respective surface areas.

MATERIALS AND METHODS

Determination of Physico-chemical Properties

The model compounds, I–IV (Fig. 1), were purchased from Sigma Chemical Co. (St. Louis, MO) and used as obtained. The properties of I were reported earlier (4). The intrinsic solubilities of II–IV were determined by placing excess material in about 10 ml solution consisting of 0.01N HCl/0.09M KCl (μ = 0.1) with a pH of 2.0 and equilibrating at 25°C for 48 hours. The solution was then filtered through a 0.2 μm syringe filter (Gelman Metricel) and analyzed by HPLC as described later. The solubilities of I–IV were also determined in the presence of one another to ensure that there is no interaction between the compounds.

The aqueous diffusion coefficients of II–IV were estimated by measuring the dissolution rates of 100% slabs of the respective compounds using the laminar dissolution apparatus as a function of flow rate and fitting the data with the analytical convective-diffusion model (13).

The densities of compressed pure compounds were determined by a solvent displacement method using water as the solvent (21). The circular pellets were made with a 0.635 cm diameter infrared punch and die (Coleman Products, England) by compressing at 51000 psi using a hydraulic press (Carver Press, Fred Carver, NJ).

HPLC Assay Methods for the Model Compounds

The HPLC assays were developed using an ODS Hypersil C18, 5 mm column with a flow rate of 1 ml/min and ambient temperature. Compounds I and II were analyzed simultaneously with a mobile phase consisting of acetonitrile–0.05 M phosphate buffer, adjusted to pH 7.0 (32:68 v/v) along with 5 mM TBA and detection at 220 nm, with a retention volume of 6.0 ml and 8.4 ml respectively. Compounds III and IV were analyzed with a mobile phase consisting of acetonitrile–0.05 M phosphate buffer, pH 7.0 (30:70 v/v) and detection at 257 nm with a retention of 2.3 ml and 5.3 ml respectively.

Preparation of Co-compressed Slabs

The compounds were compressed, crushed and sieve graded to obtain particles of limited size range. They were then passed through sieve numbers 40, 60, 80, 100 and 200 (Newark Wire Cloth Company, Newark, NJ). Particles collected on sieves 60, 80 and 200 had a nominal particle size of

335 μm, 214 μm and 112 μm respectively, based on sieve analysis (22). These nominal particle sizes were assumed for model purposes. It can be seen in the results section that the particle size within the range of sieve analysis does not affect the dissolution rate significantly. Compounds I and II with identical particle size ranges were mixed together with ratios of 10:90, 25:75, 50:50, 75:25 and 90:10. Similar mixtures were also made with III and IV. Random samples of these mixtures were analyzed by HPLC as described above, in order to ensure complete and random mixing of the particles. Rectangular slabs with dimensions of 1.575 cm × 0.32 cm were made from these mixtures on a hydraulic press (Carver Press, Fred Carver, NJ) at 51000 psi using the punch and die as described earlier (16).

Determination of Dissolution Rates

The dissolution studies of the co-compressed slabs (I/II and III/IV) were performed as reported earlier using the laminar flow cell with the long axis of the slab parallel to the flow (13). Each slab was used for one run only. The bulk solution consisting of 0.01N HCl/0.09M KCl (μ = 0.1), pH 2.0, was pumped through the cell at a set flow rate using a syringe infusion pump (Sage Instruments). The effluent was collected in a beaker and samples were withdrawn at regular intervals from the beaker. The samples were analyzed by HPLC as described above. The dissolution run was stopped after 10 minutes when steady-state was reached. Dissolution rate was calculated from the steady-state concentration of the dissolved material and volumetric flow rate of the bulk solution. The effects of flow rate and particle size on dissolution from the co-compressed slabs consisting of I and II were studied, while dissolution studies on co-compressed slabs consisting of III and IV were done at a flow rate of 3.45 ml/min and particle size of 112 μm.

RESULTS AND DISCUSSION

Physico-chemical Properties of the Model Compounds

The dissolution rates of pure slabs of the model compounds II–IV in the laminar dissolution apparatus are listed in Table II. From a convective-diffusion model reported earlier for pure neutral compounds, an expression was developed to calculate dissolution rates as indicated by Eq. 2 below (13):

$$R = \left(\frac{1.468\ D^{2/3}\ C_o\ b\ L^{2/3}}{(H^2\ W)^{1/3}} \right) Q^{1/3} \qquad (2)$$

where D is the diffusion coefficient, C_o is intrinsic solubility, b and L are slab dimensions, H and W are channel dimensions and Q is the flow rate. The equation can be modified to a linear form as follows for estimation of the diffusion coefficient from the intercept:

$$\text{Log R} = \text{Log} \left(\frac{1.468\ D^{2/3}\ C_o\ b\ L^{2/3}}{(H^2\ W)^{1/3}} \right) + 0.33\ \text{Log Q} \qquad (3)$$

A linear fit on log-log plots of dissolution rate versus the flow rate for the data in Table II resulted in the following equations for compounds II–IV respectively:

$$\text{Log } R_{II} = -9.393 + 0.385\ \text{Log Q} \qquad r^2 = 1.00$$
$$\text{Log } R_{III} = -8.325 + 0.331\ \text{Log Q} \qquad r^2 = 0.99$$
$$\text{Log } R_{IV} = -8.534 + 0.38\ \text{Log Q} \qquad r^2 = 0.99$$

The diffusion coefficients of II–IV were estimated from the intercepts using the solubilities determined experimentally (Table III) and from the slab and channel dimensions.

The intrinsic solubilities, slab densities and the estimated diffusion coefficients for all the model compounds are listed in Table III. The intrinsic solubilities of the compounds were not affected by the presence of each other and so were determined to be non-interacting.

Comparison of Dissolution Rates from Co-compressed Slabs with the Higuchi Model:

As indicated earlier, a model was proposed by Higuchi et al. (6) for the dissolution from multi-component slabs. That model assumed a simple diffusion layer theory and diffusion controlled dissolution based on Noyes-Whitney relationship. Convective transport was neglected in the model which resulted in a simple one-dimensional steady-state equation. The dissolution rates were calculated for the laminar system using Higuchi's model for various proportions of A and B so that it can be compared to the numerical convective-diffusion model. The diffusional film length of the components were calculated from the experimental dissolution rate of the compounds from pure slabs at a flow rate of 3.45 ml/min in the laminar dissolution cell and Noyes-Whitney relationship and listed in Table III. An average film

TABLE II. Experimentally determined dissolution rates (mean ± s.d., n = 3) from the pure pellets of the model compounds as a function of flow rate in the laminar dissolution apparatus. The diffusion coefficients of the compounds can be estimated from the log-log plot of dissolution rate vs the flow rate as described in Ref. 13.

Flow rate, Q (ml/min)	Phenytoin Dissolution Rate, R ($\times 10^{10}$ moles/min)	Hydrocortisone Dissolution Rate, R ($\times 10^{9}$ moles/min)	Nitrofurantoin Dissolution Rate, R ($\times 10^{9}$ moles/min)
1.10	4.19 ± 0.13	4.86 ± 0.14	3.02 ± 0.34
3.45	6.52 ± 0.10	7.21 ± 0.24	4.69 ± 0.13
5.10	7.54 ± 0.09	8.16 ± 0.08	5.61 ± 0.18
8.49	9.21 ± 0.04	9.50 ± 0.06	6.59 ± 0.06

TABLE III. Experimentally determined physico-chemical properties of the model compounds, unless otherwise indicated, at 25°C and ionic strength adjusted to 0.1 using potassium chloride.

Model Compounds	Solubility (M)	pKa	Diffusion Coefficient (cm^2/sec)	Pellet Density (g/cm^3)	Diffusional Film Thickness[d] (cm)
Naproxen (I)[a]	1.37×10^{-4}	4.57	3.90×10^{-6}	1.27	0.023
Phenytoin (II)	7.31×10^{-5}	8.17[b]	8.19×10^{-6}	1.17	0.028
Hydrocortisone (III)	8.67×10^{-4}	—	7.93×10^{-6}	1.39	0.029
Nitrofurantoin (IV)	4.19×10^{-4}	7.20[c]	1.16×10^{-5}	1.60	0.030

[a] All data listed for naproxen obtained from Ref. 17
[b] Data from Ref. 23
[c] Data from Ref. 24
[d] Calculated for a flow rate of 3.45 ml/min

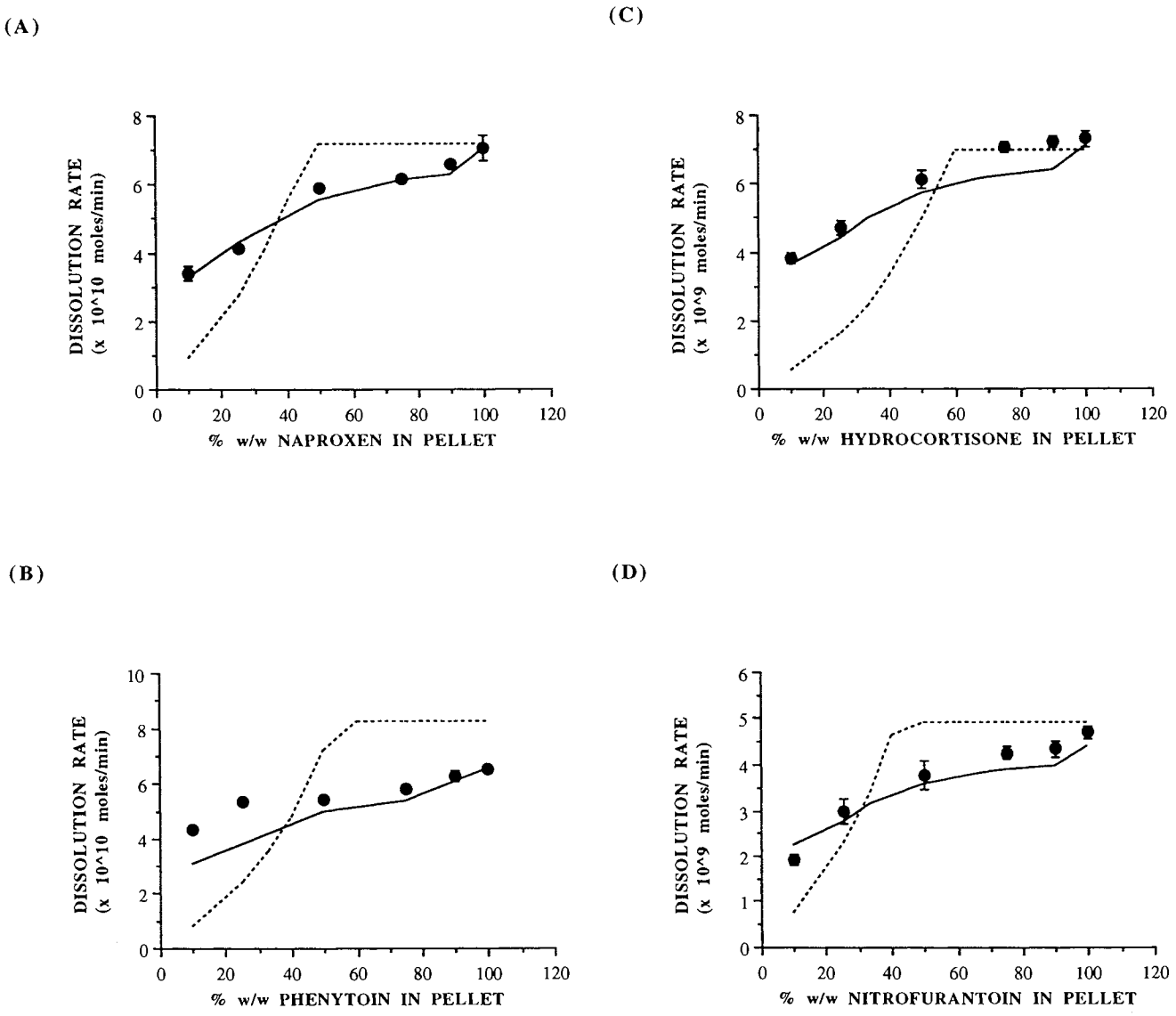

Figure 3 Comparison of the experimental dissolution rate profiles of the model compounds as a function of the weight proportion in the pellet (●) to the model proposed by Higuchi (---) and to the numerical model for the present study (—) at 3.45 ml/min and 112 μm. (A) Naproxen (B) Phenytoin (C) Hydrocortisone and (D) Nitrofurantoin. Error bars represent the standard deviation for three runs.

length of the two components was used to calculate Higuchi model predictions. Figure 3 indicates that the experimental data correlate poorly with the Higuchi model prediction along with the absence of a plateau, whereas, the convective-diffusion model predictions are quite accurate and consistent. Thus it is apparent that the exclusion of the convective transport mechanism along with perhaps other assumptions in the earlier model, may not be valid for this system.

Effects of Flow Rate and Particle Size

The effect of flow rate on dissolution for various weight proportions of naproxen and phenytoin with a nominal particle size of 112 μm and flow rates of 1.1 ml/min, 3.45 ml/min and 8.49 ml/min is shown in Figure 4. As the flow rate increased, an increase in dissolution rate was observed. A good correlation was found between the experimental and numerical dissolution rates for naproxen, while a slight deviation (about 20%) was observed at low weight proportions for phenytoin. In order to understand the role that the fluid hydrodynamics plays at different weight proportions of the components, a log-log plot of dissolution rate versus the flow rate was plotted. These plots are linear with a constant slope of around 0.33 while only the intercept changes. The cube root dependency (constant slope in the log-log plot) of the dissolution rate on the flow rate at all proportions suggests that the hydrodynamics over the sections of the components is not affected by slab composition and that the dissolution rates are modified only due to the changes in the surface area. The implications of the changes in the intercept is being explored and will be reported subsequently.

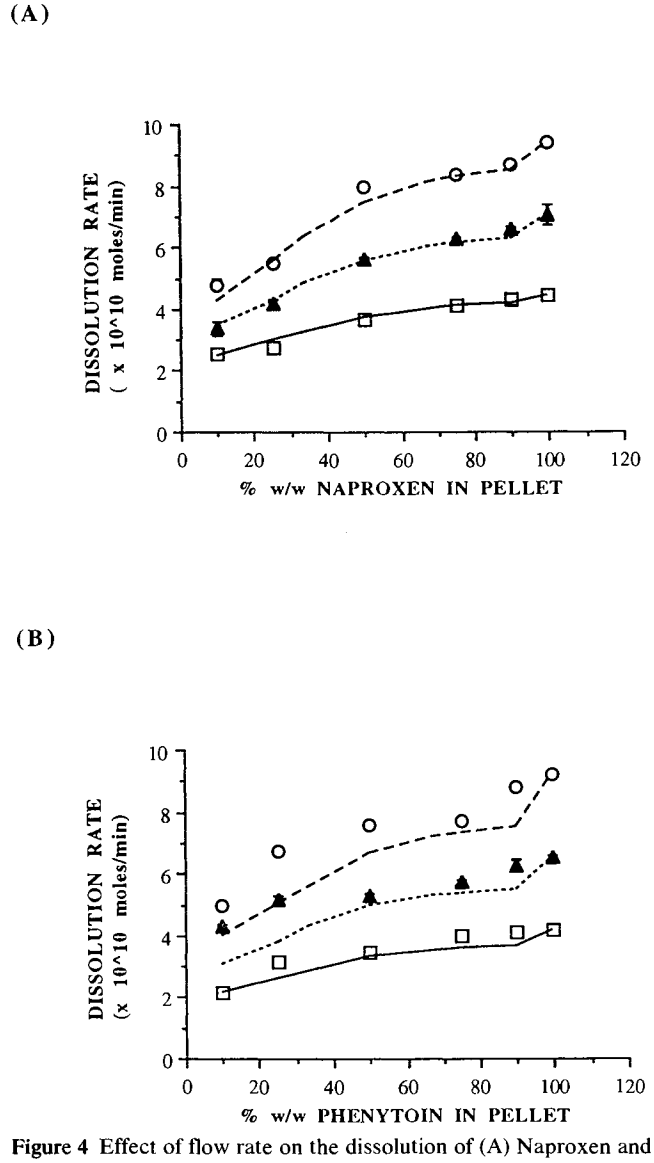

Figure 4 Effect of flow rate on the dissolution of (A) Naproxen and (B) Phenytoin from co-compressed pellets with a particle size of 112 μm; (○, - - -), 8.49 ml/min; (▲, ----) 3.45 ml/min; (□, —), 1.1 ml/min. Symbols represents experimental data and lines represents numerical model results. Error bars represent the standard deviation for three runs.

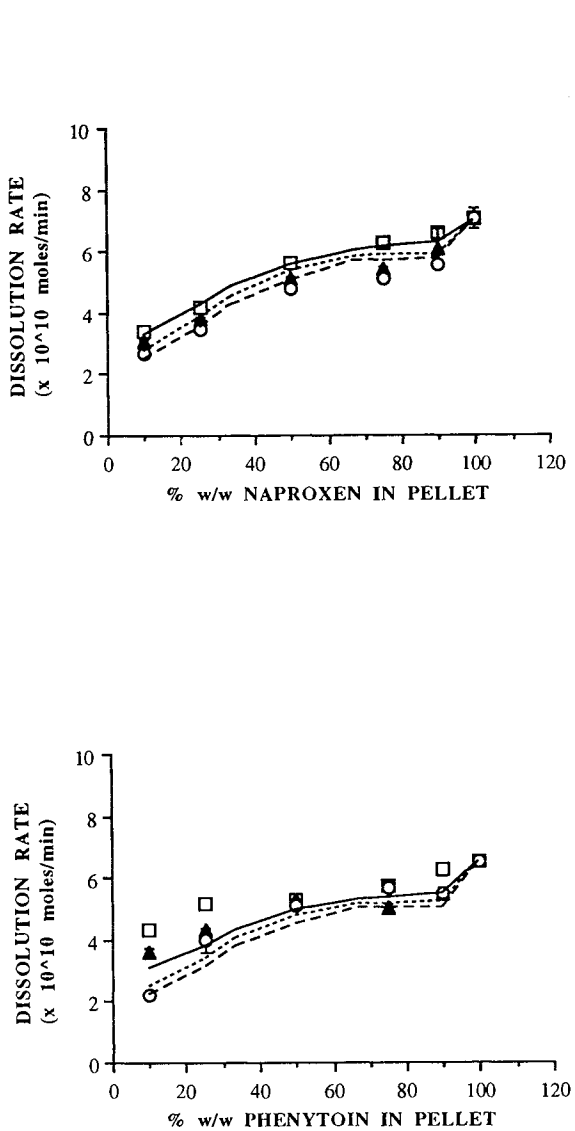

Figure 5 Effect of particle size at 3.45 ml/min for (A) Naproxen and (B) Phenytoin. (□, —), 112 μm; (▲, ----), 214 μm; (○, - - -), 335 μm. Symbols represent the experimental data and the lines represent the numerical model prediction. Error bars represent the standard deviation for three runs.

The dissolution results from co-compressed slabs of naproxen and phenytoin at a flow rate of 3.45 ml/min at varying particle sizes of 112 μm, 214 μm and 335 μm are shown in Figure 5. Once again the correlation between the experimental results and numerical values is quite good for naproxen and a relatively slight deviation observed for phenytoin at low proportions. As the particle size is increased, a decrease in dissolution rate is observed. The probable explanation for this effect is discussed below with the 'carryover' phenomena. The model simulation using extreme particle sizes for particles collected in sieve no. 60 (250 μm and 420 μm) indicated less than 10% variation in the calculated dissolution rates at 10% w/w of the component in the slab (where maximum differences were observed). This justifies the assumption of the nominal particle size for each range of particles studied.

The simulated concentration profiles for naproxen shown in Figure 6 suggest that material from the section occupied by A (naproxen, in this case) is carried over to the adjacent section occupied by B and also into the next section occupied by A, due to convection. For the 25% case, the section occupied by B is more than that of A and it acts as a sink for the material dissolving out of section A. This results in a higher concentration gradient and hence more transport. Since diffusion is a concentration driven process, this effectively increases the dissolution rate from the dissolving surface and hence the flux. In the 75% case, more material is carried over to the next section of A since the section that B occupies is smaller, resulting in a lower flux of A. The explanation for the effect of particle size can be done similarly, since the component lengths L1 and L2 increase with an increase in the particle size resulting in greater 'carryover' and hence lower flux.

Limitations of the Model

When numerical methods are employed to solve differential equations, errors are introduced with finite difference

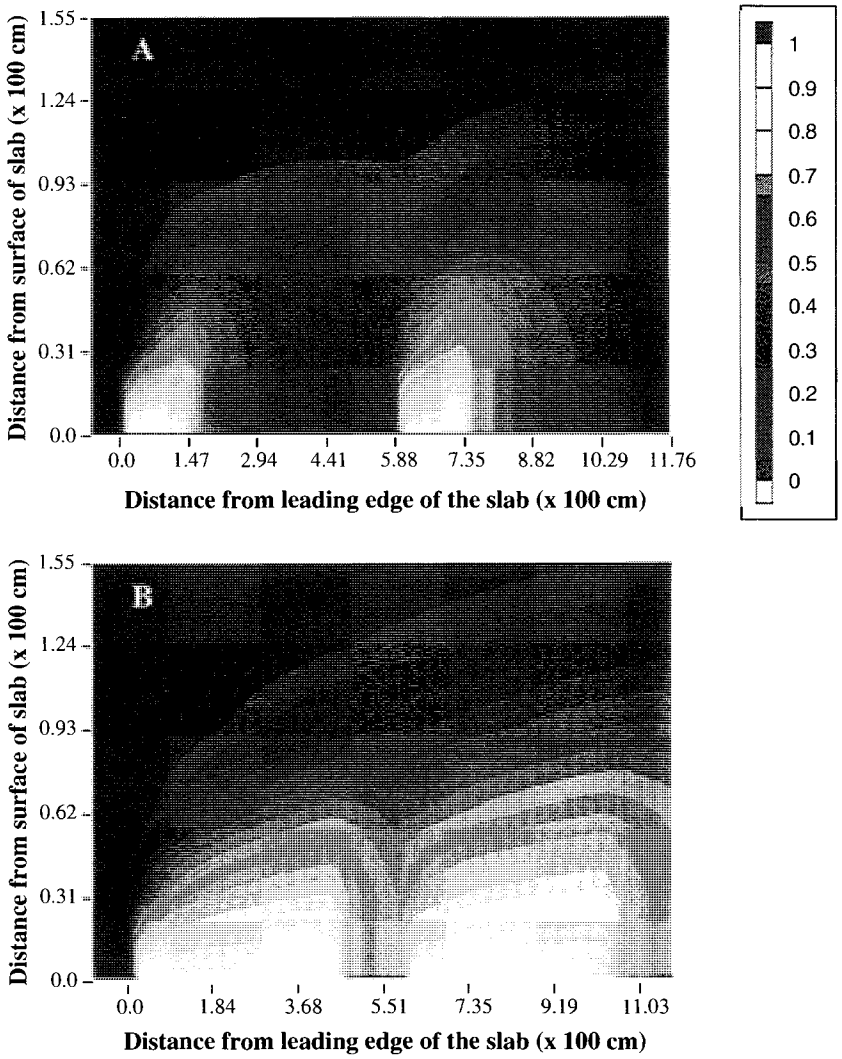

Figure 6 Simulated concentration profiles for naproxen from co-compressed pellet at (A) 25% w/w in pellet and (B) 75% w/w in pellet. The concentrations were normalized with respect to saturated solubility and range from saturated solubility (1, lighter section) at the surface to sink conditions (0, darker section) in the bulk solution.

approximations. In this study, these errors were minimized by using higher order implicit approximations (19). To obtain reproducible experimental values for the dissolution rates, the dissolving compounds should both be sparingly soluble in water and have similar solubility. Otherwise, the compound(s) with higher solubility will dissolve quickly, causing uneven erosion of the surface and/or pitting. This will introduce local eddy currents and disrupt the laminar hydrodynamics of the system. For example, the worst agreement between the model and the experimental data seen at low phenytoin weight proportion may probably be because of the pitting caused by the more soluble naproxen. The current model does not account for these effects.

An attempt was made to model dissolution from co-compressed slabs in a rotating disk hydrodynamic system (18). Because of the 'carry-over', the radial transport could not neglected and the transport equations get quite complicated. For ease of computation, several assumptions had to be made with respect to fluid flow, such as negligible axial convection. Also, the circular geometry of the dissolving surface required several approximations to be made to simplify the system. Because of the inaccuracy of these assumptions, the model prediction of the experimental results was more qualitative than quantitative. With the present laminar flow system such assumptions are avoided, enabling a better representation of the physical process.

CONCLUSION

A numerical model has been proposed to describe the dissolution of two neutral, non-interacting compounds co-compressed into a slab under laminar flow hydrodynamics. The model takes both convective and diffusive transport mechanisms into account. The ability of the model to predict the experimental results has been found to be quite accurate, to within 7%, for all the model compounds studied, except for phenytoin at low weight proportions. This model prediction was also found to be much better than an earlier model proposed by Higuchi et al. (6), which assumed a simple diffusion layer theory and neglected convective transport, suggesting that convective transport plays an important role in drug dissolution.

The effects of flow rate and particle size were studied with co-compressed slabs of naproxen and phenytoin. The results indicated that the dissolution rates of the compounds were affected by the changes in the surface area occupied in the slab. Also, the model demonstrated the effects of solute 'carryover' due to convective transport on the concentration profile near the slab surface.

The present study demonstrates unequivocally that both fluid dynamics and diffusion within the boundary layer close to the dissolving surface affect the rate of dissolution. This becomes a crucial factor when the dissolving materials in the formulation interact with one another. Studies are currently underway to extend this model to interacting species such as buffers and ionizable drugs such as weak acids and bases to explore this phenomenon further.

ACKNOWLEDGMENTS

This work was supported by the Center for Drug Delivery Research, a member of the Higuchi Biosciences Center, a Kansas Technology Enterprise Corporation Center for Excellence and by Grant GM-47848 from the National Institutes of Health. The authors wish to acknowledge Dr. Ashok Shah, UpJohn Company, Kalamazoo, MI, for providing his laminar dissolution apparatus.

REFERENCES

1. A. W. Hixson and S. J. Baum. Mass transfer and chemical reaction in liquid-solid agitation. *J. Ind. Eng. Chem.* 35:528. (1944)
2. C. V. King and S. S. Brodie. The rate of dissolution of benzoic acid in dilute aqueous alkali. *J. Am. Chem. Soc.* 59:1375–1379. (1937)
3. K. G. Mooney, M. A. Mintun, K. J. Himmelstein and V. J. Stella. Dissolution kinetics of carboxylic acids I: Effect of pH under unbuffered conditions. *J. Pharm. Sci.* 70:13–22. (1980)
4. D. P. McNamara and G. L. Amidon. Dissolution of acidic and basic compounds from the rotating disk: Influence of convective diffusion and reaction. *J. Pharm. Sci.* 75:858–868. (1986)
5. M. Z. Southard, D. W. Green, V. J. Stella and K. J. Himmelstein. Dissolution of ionizable drugs into unbuffered solution: A comprehensive model for mass transport and reaction in the rotating disk geometry. *Pharm. Res.* 9(1):58–69. (1992)
6. W. I. Higuchi, N. A. Mir and S. J. Desai. Dissolution rates of polyphase mixtures. *J. Pharm. Sci.* 54(10):1405–1410. (1965)
7. S. A. Shah and E. L. Parrott. Dissolution of two-component solids. *J. Pharm. Sci.* 65(12):1784–1790. (1976)
8. G. R. Carmichael, S. A. Shah and E. L. Parrott. General model for dissolution rates of n-component, non disintegrating spheres. *J. Pharm. Sci.* 70(12):1331–1338. (1981)
9. A. M. Healy and O. I. Corrigan. Predicting the dissolution rate of ibuprofen-acidic excipient compressed mixtures in reactive media. *Int. J. Pharm.* 84:167–173. (1992)
10. D. P. McNamara and G. L. Amidon. Reaction plane approach for estimating the effects of buffers on the dissolution rates of acidic drugs. *J. Pharm. Sci.* 77(6):511–517. (1988)
11. J. Hirtz. The gastro-intestinal absorption of drugs in man: A review of current concepts and methods of investigation. *Br. J. Clin. Pharmacol.* 19:77S. (1985)
12. J. Dainty. Water relations of plant cells. *Adv. Bot. Res.* 1:279. (1963)
13. A. C. Shah and K. G. Nelson. Evaluation of a convective diffusion drug dissolution rate model. *J. Pharm. Sci.* 64(9):1518–1520. (1975)
14. K. G. Nelson and A. C. Shah. Convective diffusion model for a transport-controlled dissolution rate process. *J. Pharm. Sci.* 64(4):610–614. (1975)
15. R. B. Bird, W. E. Stewart and E. N. Lightfoot. *Transport Phenomena*. John Wiley & Sons, New York, 1975.
16. S. Neervannan, J. D. Reinert, V. J. Stella and M. Z. Southard. A numerical convective-diffusion model for dissolution of neutral compounds under laminar flow conditions. *Int. J. Pharm.* 96:167–174 (1993).
17. Y. A. Schreider. *The monte carlo method, The method of statistical trials*. Pergamon Press, New York, 1966.
18. L. S. J. Dias. *Dissolution of weak acids from the rotating disc apparatus: Modifications by buffers and surface area availability*. Ph. D Dissertation, The University of Kansas, Lawrence, 1990.
19. B. Carnahan, H. A. Luther and J. O. Wilkes. *Applied numerical methods*. John Wiley & Sons, New York, 1969.
20. S. C. Chapra and R. P. Canale. *Numerical methods for engineers—Second Edition.*, McGraw Hill, New York, 1988.
21. S. C. Martin, J. Swarbrick and A. Cammarata. *Physical pharmacy*. 3rd ed., Lea & Febiger, Philadelphia, PA, 1983.
22. *Remington's Pharmaceutical Sciences*. 17th ed., Mack Publishing Company, Easton, PA, 1985
23. A. S. Kearney. *Evaluation of pharmaceutical potential of phosphate monoester prodrugs*. Ph.D. Dissertation, The University of Kansas, Lawrence, 1990.
24. *The Merck Index*. 11th edition, Merck and Co., Inc., Rahway, New Jersey, 1989.